

Design and Simulation of Photovoltaic Water Pumping System

Rakesh Kumar¹, Girish K. Dalal²

¹Mewar University, Department of Electrical Engineering, Chittorgarh, Rajasthan, India

²Mewar University, Department of Electrical Engineering, Chittorgarh, Rajasthan, India

Abstract: This Paper deals with the design and simulation of a simple but efficient photovoltaic water pumping system. It provides theoretical studies of photovoltaic and modeling techniques using equivalent electric circuits. The system employs the maximum power point tracker (MPPT). The investigation includes discussion of various MPPT algorithms and control methods. PSpice simulations verify the DC-DC converter design. MATLAB simulations perform comparative tests of two popular MPPT algorithms using actual irradiance data. The thesis decides on the output sensing direct control method because it requires fewer sensors. This allows a lower cost system. Each subsystem is modeled in order to simulate the whole system in MATLAB. It employs SIMULINK to model a DC pump motor, and the model is transferred into MATLAB. Then, MATLAB simulations verify the system and functionality of MPPT. Simulations also make comparisons with the system without MPPT in terms of total energy produced and total volume of water pumped per day. The results validate that MPPT can significantly increase the efficiency and the performance of PV water pumping system compared to the system without MPPT.

Keywords: MATLAB/Simulink, PSpice, MPPT.

1. Introduction

A water pumping system needs a source of power to operate. In general, AC powered system is economic and takes minimum maintenance when AC power is available from the nearby power grid. However, in many rural areas, water sources are spread over many miles of land and power lines are scarce. Installation of a new transmission line and a transformer to the location is often prohibitively expensive. Today, many stand-alone type water pumping systems use internal combustion engines. These systems are portable and easy to install. However, they have some major disadvantages, such as: they require frequent site visits for refueling and maintenance, and furthermore diesel fuel is often expensive and not readily available in rural areas of many developing countries. The consumption of fossil fuels also has an environmental impact, in particular the release of carbon dioxide (CO₂) into the atmosphere. CO₂ emissions can be greatly reduced through the application of renewable energy technologies, which are already cost competitive with fossil fuels in many situations. PV systems are highly reliable and are often chosen because they offer the lowest life-cycle cost, especially for applications requiring less than 10KW, where grid electricity is not available and where internal-combustion engines are expensive to operate. If the water source is 1/3 mile (app. 0.53Km) or more from the power line, PV is a favorable economic choice.

2. Water Pump

Two types of pumps are commonly used for PV water Pumping applications: positive displacement and centrifugal [1]. Positive displacement types are used in low-volume pumps [2] and cost-effective. Centrifugal pumps have relatively high efficiency and are capable of pumping a high volume of water. A typical size of system with this type pump is at least 500W or larger. DC motors are preferred

because they are highly efficient and can be directly coupled with a PV module or array. Brushed types are less expensive and more common although brushes need to be replaced periodically (typically every two years). There is also an aforementioned brushless type. The water pump chosen here for its size and cost is the Kyocera SD 12-30 submersible solar pump. It is a diaphragm-type positive displacement pump equipped with a brushed permanent magnet DC motor and designed for use in standalone water delivery systems, specifically for water delivery in remote locations. Flow rates up to 17.0L/min (4.5GPM) and heads up to 30.0m (100ft.) [2]. The typical daily output is between 2,700L and 5,000L. The rated maximum power consumption is 150W. It operates with a low voltage (12~30V DC), and its power requirement is as little as 35W [2].

3. MPPT Controller

Analog controllers have traditionally performed control of MPPT. However, the use of digital controllers is rapidly increasing because they offer several advantages over analog

Controllers. First, digital controllers are programmable thus capable of implementing advanced algorithm with relative ease. It is far easier to code the equation, $x = y \times z$, than to Design an analog circuit to do the same. For the same reason, modification of the design is much easier with digital controllers. They are immune to time and temperature drifts because they work in discrete, outside the linear operation. As a result, they offer long-term stability. They are also insensitive to component tolerances since they implement algorithm in software, where gains and parameters are consistent and reproducible. They allow reduction of parts count since they can handle various tasks in a single chip. Many of them are also equipped with multiple A/D converters and PWM generators, thus they can control multiple devices with a single controller.

3.1 I-V curves of BP SX 150S PV module

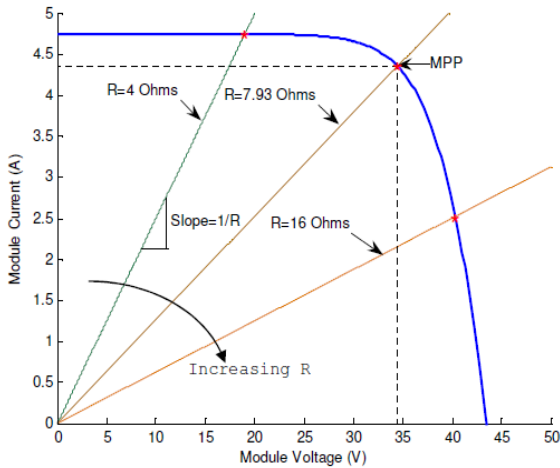


Figure 1: I-V curves of BP SX 150S PV module and various resistive loads Simulated with the MATLAB model (1KW/m2, 25oC)

3.2 I-V Characteristics of DC Motors

A permanent magnet DC (PMDC) motor is preferred in PV systems because it can provide higher starting torque. Figure 2 shows an electrical model of a PMDC motor. When the motor is turning, it produces a back emf, or a counter electromotive force, described as an electric potential (E) proportional to the angular speed of the rotor. From the equivalent circuit, the DC voltage equation for the armature circuit is:

$$V = I \times R + K \times \omega$$

Where: R_a is the armature resistance. The back emf is $E = K \cdot \omega$ where: K is the constant, and ω is the angular speed of rotor in rad/sec.

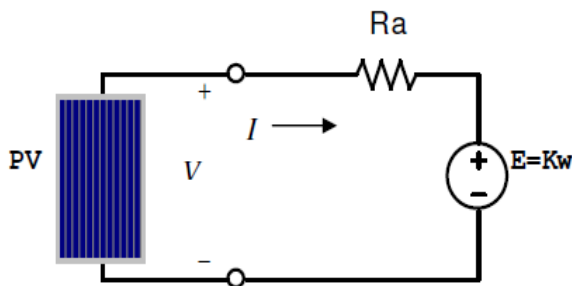


Figure 2: Electrical model of permanent magnet DC motor

Applying the voltage to start the motor, the current rises rapidly with increasing voltage until the current is sufficient to create enough starting torque to break the motor loose from static friction. At start-up, there is no effect of back emf, therefore the starting current builds up linearly with a steep slope of I/R_a on the I - V plot as shown in Figure 3-4. Once it starts to run, the back emf takes effect and drops the current, therefore the current rises slowly with increasing voltage.

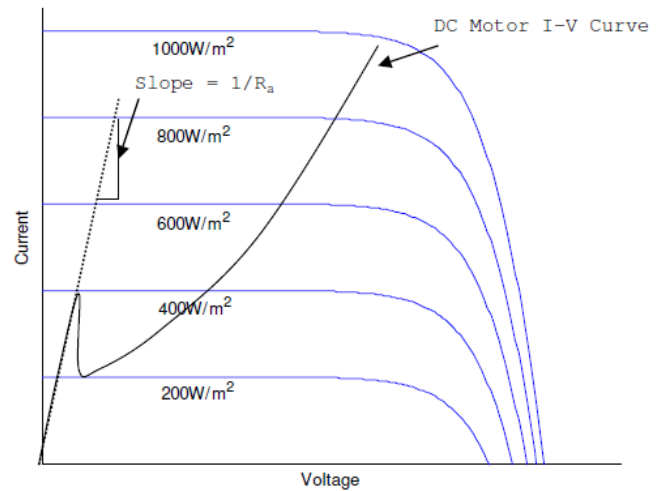


Figure 3: PV I-V curves with iso-power lines (dotted) and a DC motor I-V curve

3.3 Cúk and SEPIC Converters

For water pumping systems, the output voltage needs to be stepped down to provide a higher starting current for a pump motor. The buck converter is the simplest topology and easiest to understand and design, however it exhibits the most severe destructive failure mode of all configurations [3]. Another disadvantage is that the input current is discontinuous because of the switch located at the input, thus good input filter design is essential. Other topologies capable of voltage step-down are Cúk and SEPIC. Even though their voltage step-up function is optional for LCB application, they have several advantages over the buck converter. They provide capacitive isolation which protects against switch failure (unlike the buck topology) [4]. The input current of the Cúk and SEPIC topologies is continuous, and they can draw a ripple free current from a PV array that is important for efficient MPPT. Figure 4 shows a circuit diagram of the basic Cúk converter. It can provide the output voltage that is higher or lower than the input voltage. The SEPIC, a derivative of the Cúk converter, is also able to step up and down the voltage. Figure 5 shows a circuit diagram of the basic SEPIC converter. The characteristics of two topologies are very similar. They both use a capacitor as the main energy storage. As a result, the input current is continuous. The circuits have low switching losses and high efficiency [5]. The main difference is that the Cúk converter has a polarity of the output voltage reverse to the input voltage. The input and output of SEPIC converter have the same voltage polarity; therefore the SEPIC topology is sometimes preferred to the Cúk topology. SEPIC may be also preferred for battery charging systems because the diode placed on the output stage works as a blocking diode preventing an adverse current going to PV source from the battery. The same diode, however, gives the disadvantage of high-ripple output current. On the other hand, the Cúk converter can provide a better output current characteristic due to the inductor on the output stage. Therefore, the thesis decides on the Cúk converter because of the good input and output current characteristics.

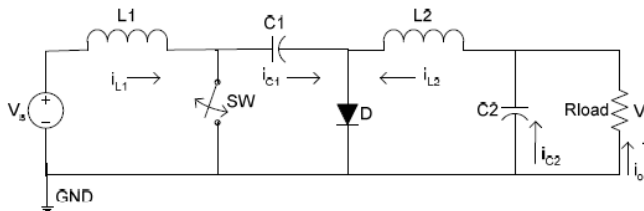


Figure 4: Circuit diagram of the basic Cuk converter

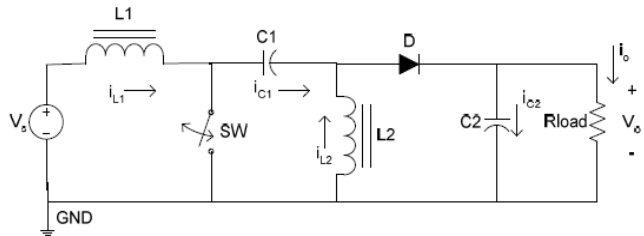


Figure 5: Circuit diagram of the basic SEPIC converter

3.4 Mechanism of Load Matching

When PV is directly coupled with a load, the operating point of PV is dictated by the load (or impedance to be specific). The impedance of load is described as below.

$$R_{load} = \frac{V_o}{I_o} \tag{1}$$

Where: V_o is the output voltage, and I_o is the output current. The optimal load for PV is described as:

$$R_{opt} = \frac{V_{MPP}}{I_{MPP}} \tag{2}$$

Where: V_{MPP} and I_{MPP} are the voltage and current at the MPP respectively. When the value of R_{load} matches with that of R_{opt} , the maximum power transfer from PV to the load will occur. These two are, however, independent and rarely matches in practice. The goal of the MPPT is to match the impedance of load to the optimal impedance of PV. The following is an example of load matching using an ideal (loss-less) Cuk converter.

$$V_s = \frac{1-D}{D} \cdot V_o \tag{3}$$

From the equation (3.10)

$$\frac{I_s}{I_o} = \frac{I_{L1}}{I_{L2}} = \frac{V_o}{V_s} \tag{4}$$

From the equation (3) and (4),

$$I_s = \frac{D}{1-D} \cdot I_o \tag{5}$$

From the equation (3) and (5), the input impedance of the converter is:

$$R_{in} = \frac{V_s}{I_s} = \frac{(1-D)^2}{D^2} \cdot \frac{V_o}{I_o} = \frac{(1-D)^2}{D^2} \cdot R_{load} \tag{6}$$

As shown in Figure 4, the impedance seen by PV is the input impedance of the Converter (R_{in}). By changing the duty cycle (D), the value of R_{in} can be matched with that of R_{opt} . Therefore, the impedance of the load can be anything as long as the duty cycle is adjusted accordingly.

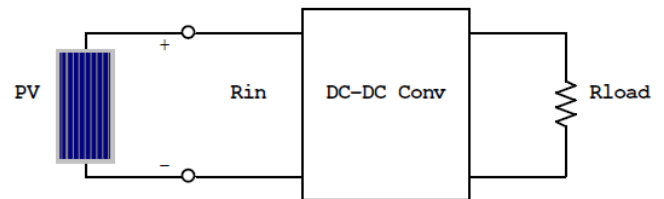


Figure 6: The impedance seen by PV is R_{in} that is adjustable by duty cycle (D)

3.5 Control of MPPT

The MPPT algorithm tells a MPPT controller How to move the operating voltage. Then, it is a MPPT controller's task to bring the voltage to a desired level and maintain it. There are several methods often used for MPPT.

3.5.1 PI Control

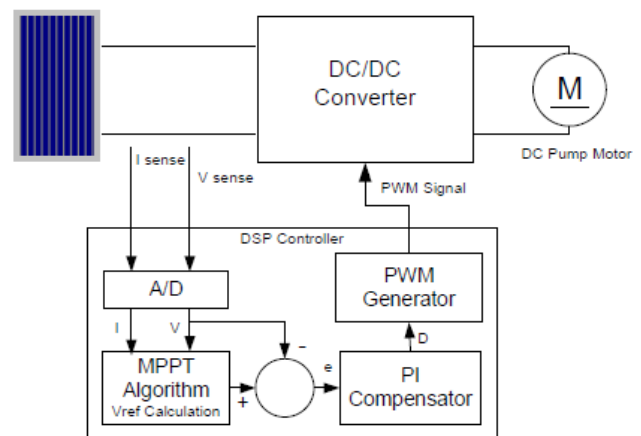


Figure 7: Block diagram of MPPT with the PI compensator

As shown in Figure 5, the MPPT takes measurement of PV voltage and current, and then tracking algorithm (P&O, incCond, or variations of two) calculates the reference voltage (V_{ref}) where the PV operating voltage should move next. The task of MPPT algorithm is to set V_{ref} only, and it is repeated periodically with a slower rate (typically 1~10 samples per second). Then, there is another control loop that the proportional and integral (PI) controller regulates the input voltage of converter. Its task is to minimize error between V_{ref} and the measured voltage by adjusting the duty cycle. The PI loop operates with a much faster rate and provides fast response and overall system stability [6] [7]. The PI controller itself can be implemented with analog components, but it is often done with DSP-based controller because the DSP can handle other tasks such as MPPT tracking thus reducing parts count.

3.5.2 Direct Control

As shown in Figure 6, this control method is simpler and uses only one control loop, and it performs the adjustment of duty cycle within the MPP tracking algorithm. The way how

to adjust the duty cycle is totally based on the theory of load matching

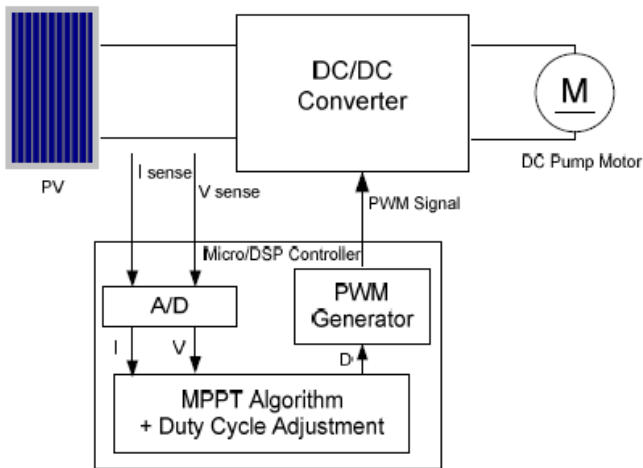


Figure 8: Block diagram of MPPT with the direct control

The impedance seen by PV is the input impedance of converter. Using the example of the Cúk converter, the relationship to the load is:

$$R_{in} = \frac{V_s}{I_s} = \frac{(1-D)^2}{D^2} \cdot R_{load} \quad (7)$$

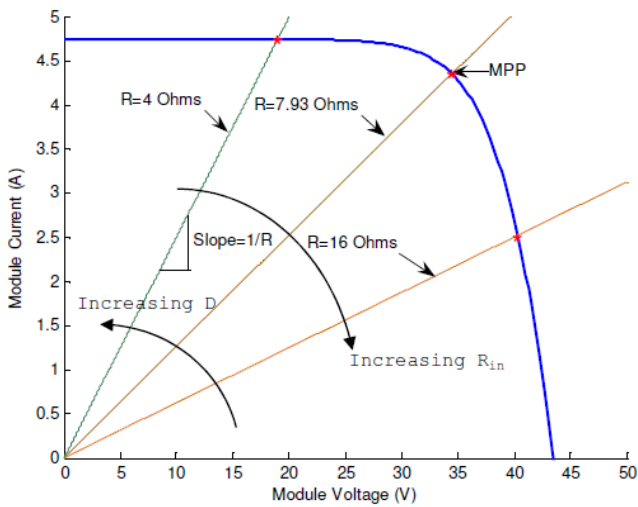


Figure 9: Relationship of the input impedance of Cúk converter and its duty cycle

where: D is the duty cycle of the Cúk converter. As shown in Figure 6, increasing D will decrease the input impedance (R_{in}), thus the PV operating voltage moves to the left. Similarly, decreasing D will increase R_{in} , thus the operating voltage moves to the right. The tracking algorithm (P&O, incCond, or variations of two) makes the decision how to move the operating voltage. The time response of the power stage and PV source is relatively slow (10~50msec depending on the type of load) [8]. The MPPT algorithm changes the duty cycle, then the next sampling of PV voltage and current should be taken after the system reaches the periodic steady state to avoid measuring the transient behavior [8]. The typical sampling rate is 10~100 samples per second. The sampling rate of PI controller is much faster,

thus it provides robustness against sudden changes of load. The system response is, however, slow in general. The direct control method can operate stably for applications such as battery equipped systems and water pumping systems. Since sampling rates are slow, it is possible to implement with inexpensive microcontrollers [7].

4. Design and Simulations

4.1 PSpice Simulations

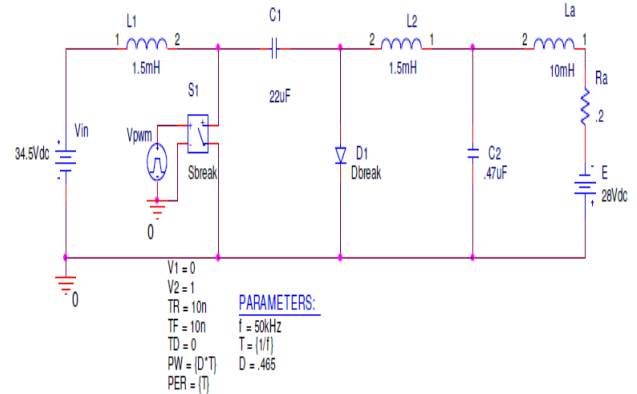


Figure 10: Schematic of the Cúk converter with PMDC motor load

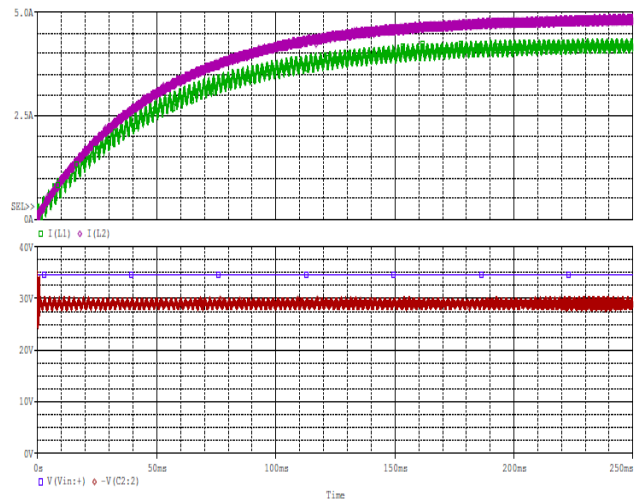


Figure 11: PSpice plots of input/output current (above) and voltage (below)

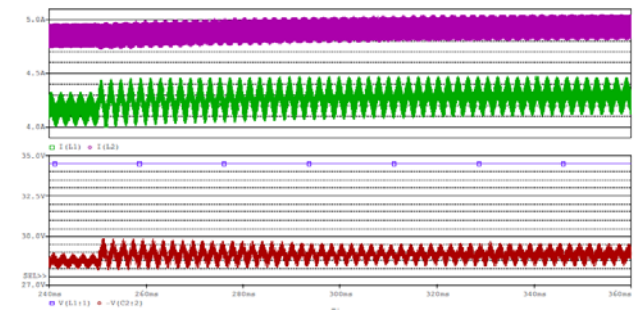


Figure 12: Transient response when duty cycle is increased 0.35% at 250ms

4.2 MPPT Simulations with DC Pump Motor Load

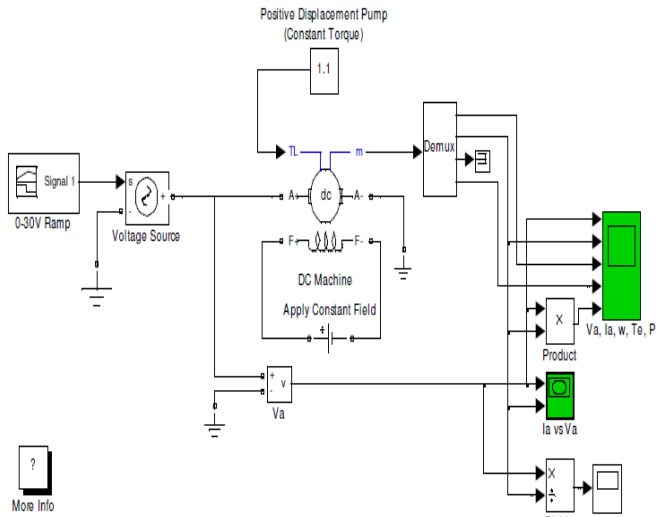


Figure 13: SIMULINK model of permanent magnet DC pump motor

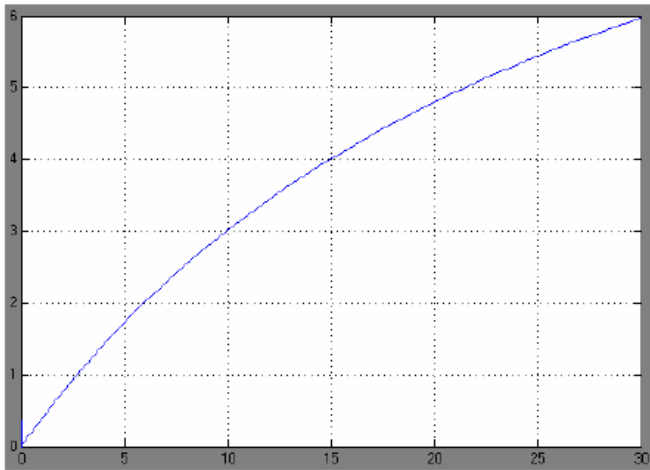


Figure 14: SIMULINK plot of Rload (Ω)

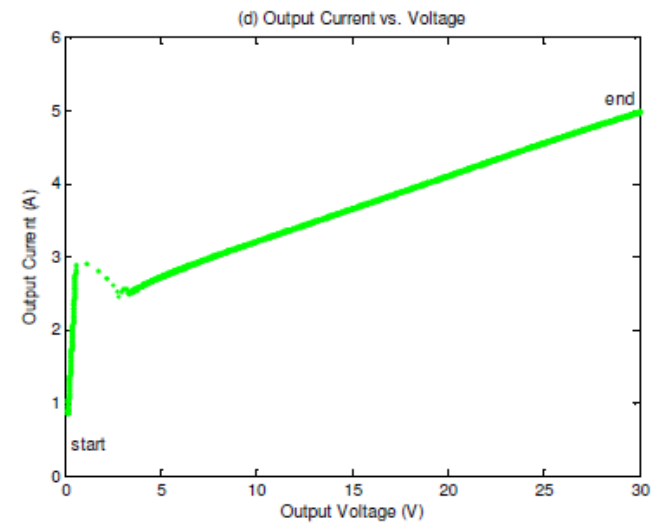
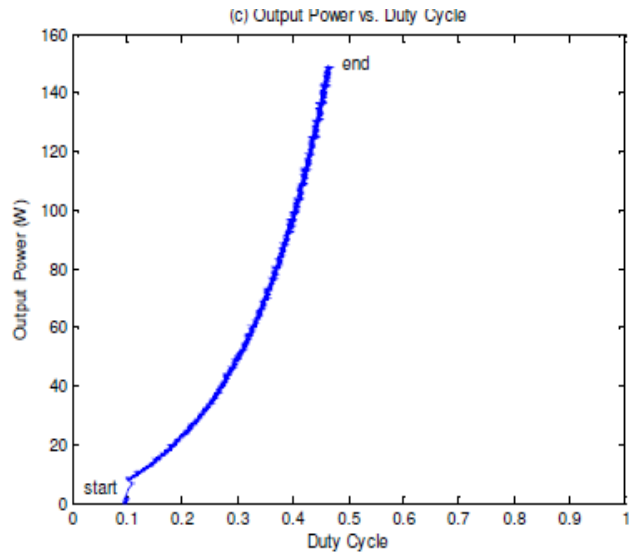


Figure 15: MPPT simulations with the DC pump motor load (20 to 1000W/m², 25oC)

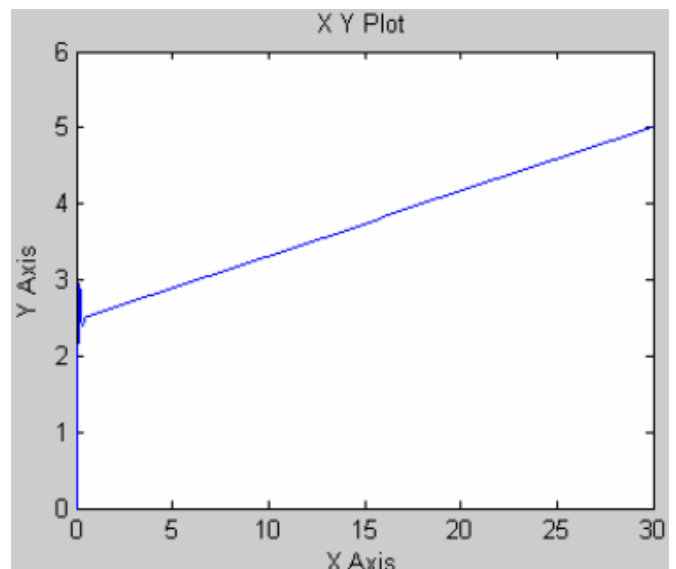
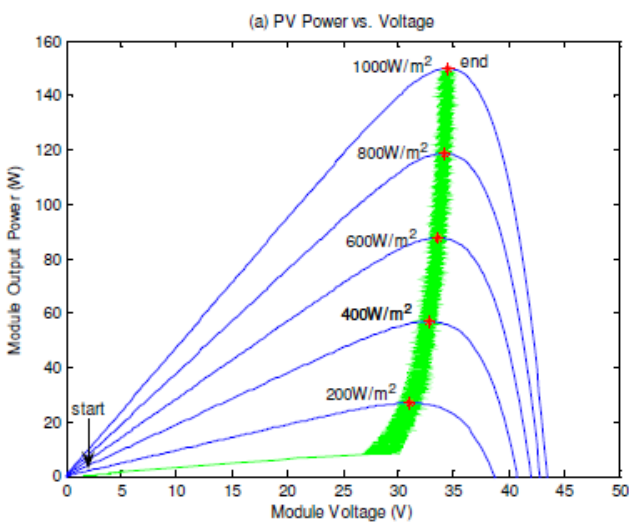


Figure 16: SIMULINK plot of DC motor I-V curve

5. Conclusion

This study presents a simple but efficient photovoltaic water pumping system. It models each component and simulates the system using MATLAB. The result shows that the PV model using the equivalent circuit in moderate complexity provides good matching with the real PV module. Simulations perform comparative tests for the two MPPT algorithms using actual irradiance data in the two different weather conditions. The incCond algorithm shows narrowly but better performance in terms of efficiency compared to the P&O algorithm under the cloudy weather condition. Even a small improvement of efficiency could bring large savings if the system is large. However, it could be difficult to justify the use of incCond algorithm for small low-cost systems since it requires four sensors. In order to develop a simple low-cost system, this thesis adopts the direct control method which employs the P&O algorithm but requires only two sensors for output. This control method offers another benefit of allowing steady-state analysis of the DC-DC converter, as opposed to the more complex state-space averaging method, because it performs sampling of voltage and current at the periodic steady state. Simulations use SimPowerSystems in SIMULINK to model a DC pump motor, and then the model is transferred into MATLAB. It performs simulations of the whole system and verifies functionality and benefits of MPPT. Simulations also make comparisons with the system without MPPT in terms of total energy produced and total volume of water pumped a day. The results validate that MPPT can significantly increase the efficiency of energy production from PV and the performance of the PV water pumping system compared to the system without MPPT.

6. Future Research

Physical implementation of the system remains for future research. It may involve implementation of: a DSP or a microcontroller, a method of supplying power to the controller, signal conditioning circuits for A/D converters, a driving circuit for Power MOSFET, a Cúk converter, and a water level sensor that detects when the water reservoir reaches full. It may also involve performance analysis on the actual system and comparisons with simulations.

References

- [1] Rashid, Muhammad H. Editor-in-Chief *Power Electronics Handbook* Academic Press, 2001
- [2] Kyocera Solar Inc. *Solar Water Pump Applications Guide* 2001 (downloaded from www.kyocerasolar.com)
- [3] Taufik *EE527 Switching Power Supply Design - Lecture Note* Cal Poly State University, San Luis Obispo, 2004
- [4] Taufik *EE410 Power Electronics I - Lecture Note* Cal Poly State University, San Luis Obispo, 2004
- [5] Rashid, Muhammad H. *Power Electronics - Circuits, Devices, and Applications 3rd Edition* Pearson Education, 2004
- [6] Hua, Chihchiang, Jongrong Lin & Chihming Shen "Implementation of a DSPControlled Photovoltaic System with Peak Power Tracking" *IEEE Transactions*

on Industrial Electronics, Vol. 45, No. 1 February 1998, page 99-107

- [7] Koutroulis, Efichios, Kostas Kalaitzakis, Nicholas C. Voulgaris "Development of a Microcontroller-Based, Photovoltaic Maximum Power Point Tracking Control System" *IEEE Transactions on Power Electronics, Vol. 16, No. 1*, January 2001, page 46-54
- [8] Hohm, D. P. & M. E. Ropp "Comparative Study of Maximum Power Point Tracking Algorithms" *Progress in Photovoltaics: Research and Applications* November 2002, page 47-62

Author Profile



Rakesh Kumar, M.Tech scholar Mewar University, Department of Electrical Engineering, Chittorgarh, Rajasthan, India

Girish K. Dalal is from Mewar University, Department of Electrical Engineering, Chittorgarh, Rajasthan, India